

Synthesis and characterisation of a potential ceramic sulfide ion conductor based on the solid solution $x\text{CaS}:\text{Nd}_2\text{S}_3$, $x = 0.7\text{--}1.0$

V. S. Johnson · K. Hellgardt · S. E. Dann ·
R. J White

Received: 2 February 2006 / Accepted: 23 October 2006 / Published online: 9 January 2007
© Springer Science+Business Media, LLC 2006

Abstract The effect of defect ion concentration on conductivity in the CaNd_2S_4 system has been investigated by varying the $\text{CaS}:\text{Nd}_2\text{S}_3$ ratio. Samples with the formula $x\text{CaS}:\text{Nd}_2\text{S}_3$, $x = 0.7\text{--}1.0$ have been prepared using solid state methods by high temperature synthesis in evacuated quartz tubes followed by annealing in hydrogen sulfide. The structures of the materials were determined using the Rietveld refinement of powder neutron diffraction data. The phases crystallise with a defect version of the cubic Th_3P_4 structure in the space group I-43d with cell parameter $a \approx 8.53 \text{ \AA}$. Temperature programmed oxidation (TPO) in a 5 Vol.% O_2/Ar atmosphere show that the materials resist oxidation up to a temperature of approximately $680 \text{ }^\circ\text{C}$. TPO also indicates that there is only one type of sulfide ion present in the system, based on the presence of only one peak in the TPO trace. In-situ impedance spectroscopy was carried out in an Ar and $\text{H}_2\text{S}/\text{Ar}$ atmosphere between $300 \text{ }^\circ\text{C}$ and $500 \text{ }^\circ\text{C}$. Bulk conductivities, activation energies and time constants for ion hopping processes were determined. The sample, $0.9\text{CaS}:\text{Nd}_2\text{S}_3$, was found to exhibit three impedance arcs in the Nyquist plot suggesting ionic conduction. The independence of the material's bulk conductivity when exposed to an $\text{H}_2\text{S}/\text{Ar}$ atmosphere supports this

statement. The $x\text{CaS}:\text{Nd}_2\text{S}_3$ sample with $x \leq 0.8$ show strong electronic contributions to the overall conductivity. The total ionic conductivity for $0.9\text{CaS}:\text{Nd}_2\text{S}_3$ of $1.09 \times 10^{-6} \text{ Scm}^{-1}$ measured at $500 \text{ }^\circ\text{C}$, matches conductivity values reported using galvanic cells.

Introduction

Fast ion conductors capable of conducting the oxide ion are relatively well-known. In contrast, only two reports have suggested compounds capable of conducting the sulfide ion, both in the MLn_2S_4 system [1–5]. This system crystallises with the Th_3P_4 structure in the space group I-43d and can withstand an unusual level of non-stoichiometry. For example, some of the lanthanide sulfides such as Sm_2S_3 form a defect version of this structure at high pressure where the cation site is only partially filled i.e. Sm_2S_3 would be written as $\text{Sm}_{2.66}\text{S}_4$. Addition of tiny amounts of CaS to the lanthanide sesquisulfides can stabilise this cubic phase at ambient temperature and pressure. Flahuat et al. [1] studied these systems in detail as a function of calcium content and these results were used by Carter to hypothesise the defect mechanisms of these materials with the formula $\text{Ca}_{1-y}\text{Ln}_2\text{S}_{4-y}$ in general [6]. At low calcium levels these materials are best described as a full sulfide lattice with partially occupied cation sites. Between $\text{Ca} = 0.3\text{--}0.8$, the materials show a mixture of defect clusters and Schottky defects. At high calcium levels a pure Schottky defect mechanism is adopted. The sulfide ion conductivity of these systems where $x = 0.7\text{--}1.0$ has been investigated using galvanic cells

K. Hellgardt (✉)
Department of Chemical Engineering and Chemical
Technology, Imperial College of Science, Technology
and Medicine, London SW7 2AZ, UK
e-mail: k.hellgardt@imperial.ac.uk

V. S. Johnson · S. E. Dann · R. JWhite
Departments of Chemical Engineering and Chemistry,
Loughborough University, Loughborough, Leicestershire
LE11 3TU, UK

[3]. The highest conductivity of $1.15 \times 10^{-6} \text{ Scm}^{-1}$ was achieved for $0.9\text{CaS:Nd}_2\text{S}_3$ with a sulfide ion transport number of 0.97 measured at 500 °C [3]. This $x = 0.9$ sample in this system has been reported to be thermally stable up to 934 °C [2].

Ionic conduction in crystalline solids requires both, ionic defects and mobile ions to move between vacant sites. For example, CeO_2 , with a fluorite structure, can be doped with rare earth oxides such as Gd_2O_3 to high levels of 10–15 mol% [7–13], which creates vacancies on the anion sublattice to which the oxygen anions can move. There is an apparent limit of effectiveness of doping however, as structures such as fluorite perturb the endless creation of random distributed vacancies by clustering them together e.g. U_4O_9 . Once clustered together, these defect clusters provide a trap for the conducting ions and ionic conductivity will fall rather than continuing to rise with the introduction of more vacancies.

There is a sparse body of information on the effect of doping of sulfide electrolytes such as CaS [5, 13–15]. In pure CaS, at least one calcium vacancy is associated with each sulfur vacancy [13] (implying Schottky defects). Ionic conductivity was confirmed in CaS at H_2S partial pressures of less than 10^{-6} atm [13]. Doping of CaS with Y_2S_3 up to 16 mol% leads to a reduction in the lattice parameter and cationic vacancies as the divalent calcium is replaced by the trivalent yttrium [14]. No conductivity measurements were made to confirm the observation. However cationic conduction has also been proposed based on the shrinking of the unit cell of the CaS upon doping.

The present work describes the detailed synthesis and in depth characterisation of the solid solution $x\text{CaS:Nd}_2\text{S}_3$; $x = 0.7\text{--}1.0$ in an attempt to confirm (or refute) previously reported observations of significant sulfide ion conductivity in this system.

Experimental

Samples with $x = 0.7\text{--}1.0$ in the $x\text{CaS:Nd}_2\text{S}_3$ system were prepared by combining the metal sulfide starting materials in the correct molar proportions. The samples were ground under an argon atmosphere in a glove box in an agate pestle and mortar. These mixtures were reacted in graphite coated evacuated silica ampoules, and heated to a maximum temperature of 1,300 °C using a ramp rate of 2 °C/min and held at temperature for 24 h. The tubes were then slow-cooled to room temperature before removal. Formation of phases with the Th_3P_4 structure was confirmed by powder X-ray diffraction by comparison of data

collected in the 2θ range 10–80° with the JCPDS database card for the parent CaNd_2S_4 phase. Rietveld refinement of X-ray powder diffraction data collected over a 10–100° 2θ range using a 0.0147° 2θ step proved challenging due to the heavily dominant scattering length of neodymium over calcium and sulfur in X-ray diffraction. Therefore powder neutron diffraction data were collected on the POLARIS diffractometer at ISIS over a period of 6 h where the scattering lengths of the three elements are notably different but are the same order of magnitude. The structure was refined using two different models. In the first model, vacancies on both the cation and anion sites were incorporated into the model with the occupancies of the calcium and associated sulfur tied together to ensure that charge balance was maintained. In the second model, a full sulfide sublattice was used with the stoichiometry of the shared calcium/neodymium site adjusted to the associated vacancies as first modelled by Flahaut et al. [1]. Initially, the background parameters and lattice parameter were refined, followed by the peak shape parameters. The atomic parameters were then added, finally followed by the isotropic temperature factors. The difference in R factors generated by these two different models is so small that there is no clear preference for either model and hence the defect mechanism cannot be determined using Rietveld methods alone. However, in order for anionic conductivity to be observed, the Schottky defect model would be preferred as a full anion sublattice would preclude anion conductivity.

Temperature programmed techniques were used to characterise the $x\text{CaS:Nd}_2\text{S}_3$ system for material stability in both, oxidising and reducing atmospheres. The sulfides were heated at a rate of 10 °C/min in a 20 mm i.d. quartz furnace. A reactor (length 300 mm, inside diameter 3.8 mm, thickness 2.5 mm and volume 6 ml) containing approximately 10–20 mg of $x\text{CaS:Nd}_2\text{S}_3$ (particle size range 38–52 μ) was heated either in the presence of 14 Vol.% hydrogen/argon mixture (45 ml/min) or 6 Vol.% of air/argon mixture (60 ml/min). The gases enter and leave the reactor through ¼" Swage-lock fittings with graphite ferrules producing air tight seals, the metal sulfide being supported by quartz wool. The oxygen and hydrogen concentrations were selected such that the Mass Spectrometer was not saturated with the reactant gas while the flow rates were chosen in order to optimise the response of the system (resolution of the peaks). All gases were controlled by AALBORG 0–200 ml/min mass flow controllers, which were calibrated using a bubble flow meter. The heating rate was controlled by a WEST 6400 temperature controller, the power to the furnace

being supplied by a Wayne Kerr 0–70 V, 0–60 amps DC power supply. This allowed for precise and accurate temperature ramping. The reactant and product gases were monitored by a Quadruple Mass Spectrometer (Vacuum Generators). Once reproducibility of the TP experiment was achieved, the thermal stability of the materials in an oxidising and a reducing atmosphere as well as the extent of oxidation was determined.

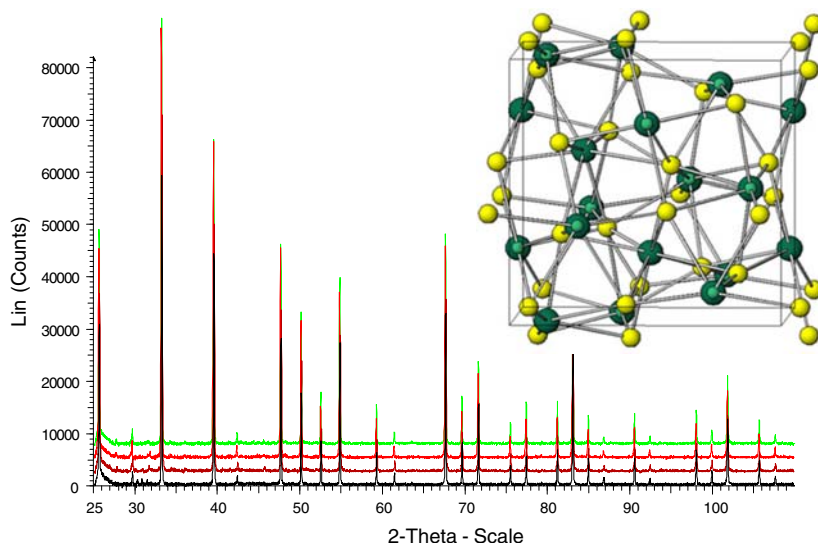
The sulfide products were ground and pressed into pellets and subsequently sintered at 1,350 °C in 10 Vol.% H₂S/H₂ (BOC) for impedance spectroscopic characterisation. The typical mass used to form a pellet was 1.4–1.5 g with a particle size range of 0.2–10 μm which gives a nominal pellet thickness of 1.35 mm and a sintered diameter of 18.5 mm. Two to four drops of liquid paraffin were used as binder. The powder and binder was mixed until small homogeneous agglomerates were obtained which then were pressed with 16 tons at room temperature. Pellets were sintered in a constant flow of 10 Vol.% hydrogen sulfide in hydrogen atmosphere, at a maximum temperature of 1,350 °C and a dwell time of 8–10 h resulting in a pellet density of 85–95% of the theoretical density. The pellets were mechanically contacted with graphite electrodes with platinum current collectors. Impedance spectroscopy (Solartron 1255 using a 1287 Dielectric Interface) was carried out in a single atmosphere reactor in argon and various hydrogen sulfide concentrations with a maximum of 2 Vol.% H₂S/Ar. Frequencies between 1 MHz and 0.01 Hz were applied at temperatures between 50 °C and 400 °C (at 50 °C intervals). An ac voltage of 0.1 V_{rms} was applied. Using appropriate modelling for pure [16] or mixed

ionic conductors [17] led to the determination of the bulk conductivity, the activation energy for ionic hopping and the time constants for the conduction process. In order to make accurate and repeatable EIS measurements, the provision of accurate temperature control was achieved with the use of a Eurotherm 2216e controller that is programmable through the impedance software provided by Solartron. This ensures that the impedance measurement does not begin until the set-point and the actual temperatures are the same, which is achieved using a dwell time of 1 h at each temperature.

Results and discussion

Rietveld analysis of neutron powder diffraction data confirmed that the series crystallises with the Th₃P₄ structure in the I-43d space group with lattice parameters very close to 8.53 Å. The structure is depicted in Fig. 1 and consists of a single cation site shared by both calcium and neodymium and a single sulfide site. In accordance with previous studies [1, 14], the cell parameter changes very little over the determined range $x\text{CaS:Nd}_2\text{S}_3$, $x = 0.7\text{--}1.0$. The X-ray diffraction patterns shown in Fig. 1 illustrate that there is no noticeable change in the lattice parameter as a function of x and the values determined by refinement of powder neutron diffraction data vary by less than 0.01 Å. This observation is contrary to Vegard's rule, which dictates that in a solid solution a smooth variation between the end members should be observed. However, the lattice parameter for $x = 0.7\text{--}1.0$ remains very close to that of the CaNd₂S₄ ($x = 1.0$) end member.

Fig. 1 Th₃P₄ Structure of CaNd₂S₄. Ca (light green)/Nd (dark green) on a shared site and S (yellow). PXRD diffraction data for $x = 0.7\text{--}1.0$



The thermal stability of the series was established using temperature programmed oxidation (TPO) and temperature programmed reduction (TPR). The TPO traces of this series consist of one major peak with a shoulder to the high temperature side, Fig. 2, with the undoped compound showing a minor peak at 825 °C. Because of its insignificant area (less than 3% of the major peak) the small peak was ignored in any mass balance calculations. The sulfur dioxide peak for this family of compounds is located in the temperature range 671–723 °C when a heating rate of 10 °C/min is applied.

The observation of one major oxidation peak indicates that there is probably only one type of sulfur present in the lattice (with a specific binding energy), which reacts and exchanges with oxygen to form sulfur dioxide. Excess sulfur (if present) would have reacted at much lower temperatures (less than 300 °C), but this was not observed. Hence a single phase may be assumed to be present in this family of compounds, which is consistent with the X-ray diffraction data. Different peak widths can be attributed to small differences in particle size distribution. From Fig. 2 it is quite clear that when x is decreased for the solid solution from 1.0 to 0.7, the onset temperature of the oxidation process as well as the peak temperature tend to shift to lower temperatures suggesting a weaker bonding of the sulfide in the lattice.

The overall decrease in TPO onset/peak temperature (the onset temperature for $x = 1.0$ being artificially low due to the rather broad nature of the peak) starting from the parent material CaNd_2S_4 may be due to the increasing disorder in the system and increasing entropy allowed easier removal of the anions. On this basis $x = 1.0$ should exhibit the highest and $x = 0.7$ the lowest onset/peak temperature. The variation in lattice parameter is unlikely to be the cause of such large variation (see Table 1).

By varying the ramp rate of the TPO experiments, thermal activation energies were extracted. These

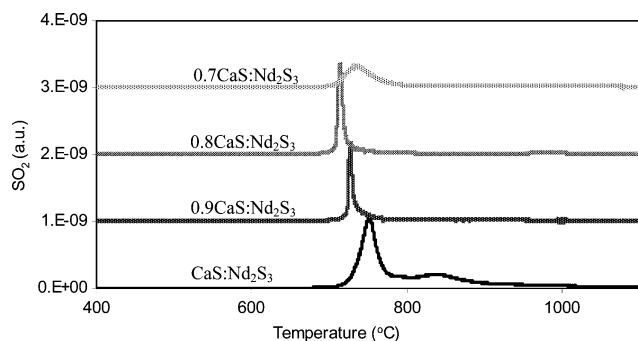


Fig. 2 TPO profiles for solid solutions $x\text{CaS:Nd}_2\text{S}_3$, $x = 0.7\text{--}1.0$

Table 1 Oxidation onset and peak temperatures as well as lattice parameter for $x\text{CaS:Nd}_2\text{S}_3$ series

	Onset temperature (°C)	Peak temperature (°C)	Thermal activation energy (J/g mol)	Lattice parameter (a-site) (Å)
$x = 1.0$	671	754	1.90×10^5	8.5301(1)
$x = 0.9$	723	726	6.37×10^5	8.5299(1)
$x = 0.8$	708	715	5.71×10^5	8.5294(1)
$x = 0.7$	703	730	4.36×10^5	8.5289(1)

range from 1.90×10^5 J/g mol to 6.37×10^5 J/g mol. It is interesting to note that the highest thermal activation energy of 6.37×10^5 J/g mol was found for the compound $0.9\text{CaS:Nd}_2\text{S}_3$. Complete sulfur balances were performed by integrating the SO_2 peak in the TPO trace, (with units a.u.·min) using appropriate SO_2 calibration curves to convert the area into molar units. The fraction of sulfur liberated from the structure, in terms of SO_2 , relative to the total sulfur present in the compound was calculated, based on the mass of sample oxidised (Eq. 1).

$$\text{Percent Oxidation} = \frac{S^{2-}_{\text{measured as SO}_2}}{S^0_{\text{moles of SO}_2}} \times 100, \quad (1)$$

where S^{2-} —moles of SO_2 liberated and measured by Mass Spectrometer; S^0 —moles of sulphur based on the mass of the sample.

It appears that the $x\text{CaS:Nd}_2\text{S}_3$ series does not form a pure oxide at 1,000 °C but all compounds seem to form a mixed oxide-sulfate system, Fig. 3. The $x = 1.0$ and $x = 0.9$ samples oxidised in a similar manner in that both compounds oxidise to form oxide or sulfate species. At lower values of x , this behaviour changes since excess sulfide apparently remains, with small amounts of oxide-sulfate present. Remarkably, galvanic cell characterisation results of Kalinina et al. [3]

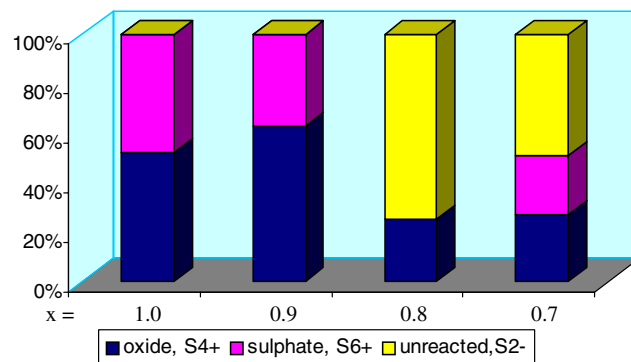


Fig. 3 Oxide and sulphate formation for $x\text{CaS:Nd}_2\text{S}_3$ series

show that $\text{CaNd}_2\text{S}_4 + 0.1\text{Nd}_2\text{S}_3$ (approximately equivalent to $x = 0.9$) has the highest sulfide ion conductivity, which also released the largest amount of sulfide from the unit cell to form SO_2 , Fig. 3. This might imply that conductivity due to mobile sulfide ions (via electrochemical activation) is related to thermally activated mobile sulfide ions (see also thermal activation data), but further investigation is needed to confirm this.

Temperature programmed reduction (TPR) of the $x\text{CaS}:\text{Nd}_2\text{S}_3$ series shows that the highest onset temperature of 766 °C is observed for $x = 0.9$ which is in agreement with the TPO experiments. All these sulfide-based materials were marginally more stable under reducing, rather than oxidising, conditions.

Mechanically contacted graphite electrodes were used during impedance spectroscopy experiments. They were chosen because gold and platinum electrodes had the tendency to react with the sulfides examined. Contact electrodes are likely to lead to spreading resistances, which in turn may cause an overlap between electrode arc and grain boundary arc. However, the high frequency arc is free from electrode effects associated with contact resistance or spreading effects [18, 19], therefore the high frequency arc should be equal to the true bulk resistance of the electrolyte, a value which should be similar to that of the single crystal.

Impedance spectroscopy data of the solid solutions $x\text{CaS}:\text{Nd}_2\text{S}_3$ with $x = 1.0, 0.8$ and 0.7 , using graphite electrodes exhibited two arcs without significant overlap so that they were easily distinguished in both the Nyquist and Bode plots. These two arcs were observed at all temperatures between 200 °C and 400 °C, Fig. 4. The solid solution $0.9\text{CaS}:\text{Nd}_2\text{S}_3$, however, exhibited three distinct arcs, including a low frequency ion blocking arc. The low frequency effect is attributed to either blocking electrodes, limiting ions to traverse the electrolyte–electrode interface or selective grain

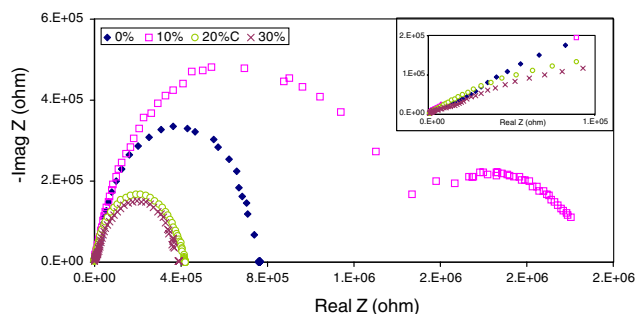


Fig. 4 Nyquist plot of CaNd_2S_4 series at 400 °C using graphite electrodes in Argon

boundary blocking. Please note that the first arc (bulk conductivity) cannot easily be seen in Fig. 4 due to the scale required for the representation of the subsequent arcs. The absence of an ionic blocking arc at low frequency occurs with materials with transport numbers as high as 0.9999 [17, 20] even though a material is considered to be an ionic conductor once the transport number for ionic conduction exceeds 0.95 [19]. Therefore the absence of the conclusive low frequency ionic blocking arc in the Nyquist diagram does not mean that the electrolyte is not predominantly ionic conducting.

Jamnik equivalent circuit models [17] for mixed conductors were used to calculate bulk properties, bulk conductivity, activation energy, and time constants of the $x\text{CaS}:\text{Nd}_2\text{S}_3$ series.

A well-researched pure oxide ion conductor is YSZ, and its activation energy for conduction lies at (or near to, depending on choice of reference) 1.25 eV. The observed range of activation energies for the $x\text{CaS}:\text{Nd}_2\text{S}_3$ series is low which infers that the CaNd_2S_4 series has mixed ionic–electronic conduction, Table 2. Activation energies for sulfide ion conductors are not readily available in the literature as there is only one reported successful synthesis attempt by Kalinina et al. [3, 4].

Galvanic cell measurements by Kalinina et al. [3] on doped CaNd_2S_4 compounds showed conductivities (at 500 °C) between 10^{-7}Scm^{-1} and 10^{-6}Scm^{-1} with $\text{CaNd}_2\text{S}_4 + 10.0 \text{ mol\% Nd}_2\text{S}_3$ (similar to $0.9\text{CaS}:\text{Nd}_2\text{S}_3$) exhibiting a value of $1.15 \times 10^{-6} \text{Scm}^{-1}$ which was the highest conductivity observed in the series.

The equivalent circuits employed to model the current impedance spectroscopy data yield much higher conductivities, Table 2. The Jamnik mixed ionic–electronic equivalent circuit identifies $0.9\text{CaS}:\text{Nd}_2\text{S}_3$ with a bulk conductivity of $1.09 \times 10^{-6} \text{Scm}^{-1}$, agreeing with Kalinina et al. [3] bulk conductivity, which was determined using galvanic cells. However, all other bulk conductivities were several orders of magnitude larger than the ones obtained by Kalinina et al. [3]. Their cell employed CaS and Nd_2S_3 discs between the electrolyte and carbon electrodes, to

Table 2 Activation energy, bulk conductivity and time constant measured at 500 °C derived from Jamnik equivalent circuit for predominant ionic conductors [17]

Material	Activation energy (eV)	Bulk conductivity (Scm^{-1})	Time constant (s^{-1})
CaNd_2S_4	0.43	2.19×10^{-8}	5.59×10^{-5}
$0.9\text{CaS}:\text{Nd}_2\text{S}_3$	0.23	1.09×10^{-6}	1.03×10^{-3}
$0.8\text{CaS}:\text{Nd}_2\text{S}_3$	0.46	3.09×10^{-5}	1.78×10^{-3}
$0.7\text{CaS}:\text{Nd}_2\text{S}_3$	0.65	1.85×10^{-5}	1.22×10^{-3}

function as ionic sources and sinks for Ca, Nd and S ions. Both, CaS and Nd₂S₃, are not electronic conductors and therefore that experimental method would not allow the conduction of electrons, and therefore cause possibly lower bulk conductivities.

Using Jamnik equivalent circuitry, time constants for bulk conduction were several orders of magnitude larger than for YSZ at similar temperatures [21], Table 2. If the basic assumption is made that a larger ion moves slower than a smaller one, then the time constants for the CaNd₂S₄ series favour anionic conduction.

Ionic conduction is also identified if the bulk conductivity is independent of the atmospheric concentration of the mobile species, in our case sulfur in the form of H₂S. Therefore impedance spectroscopy was carried out from 350 °C to 550 °C with concentrations of H₂S/Ar varying from 18 Vol.% to 0.1 Vol.% at each temperature. One hour isothermal periods allowed temperatures and concentrations to stabilise prior to impedance measurements.

Results for the *x*CaS:Nd₂S₃ series show that the conductivity depends on the H₂S concentration, Fig. 5, and increases with increasing sulfur concentration. The onset of hole conduction may occur at high H₂S concentration according to Eq. 2.



where $V_{S^{2-}}$ —sulphide anion vacancy; S^{2-} —sulphur anion in unit cell; \oplus —electron hole.

Thus, increasing the sulfur partial pressure increases the number of electron holes and thereby increases the conductivity of the *x*CaS:Nd₂S₃ electrolyte. Interestingly, hole conduction dominates calcium sulfide behaviour at partial pressures greater than $\log(P_{S_2}) = -6$, at lower partial pressures, ionic conduction prevails [13].

The conductivity of 0.9CaS:Nd₂S₃ appears to be independent of the H₂S partial pressure at temperatures

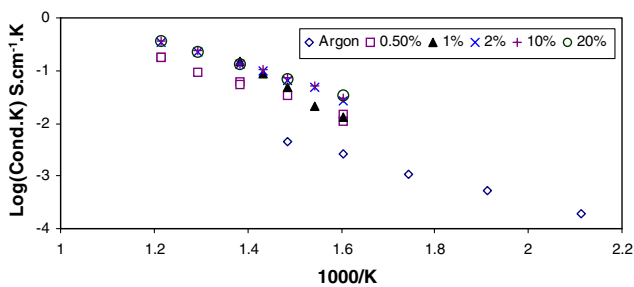


Fig. 5 Concentration dependency of bulk conductivity versus temperature for undoped CaNd₂S₄. The legend gives the H₂S concentration in hydrogen in Vol.%

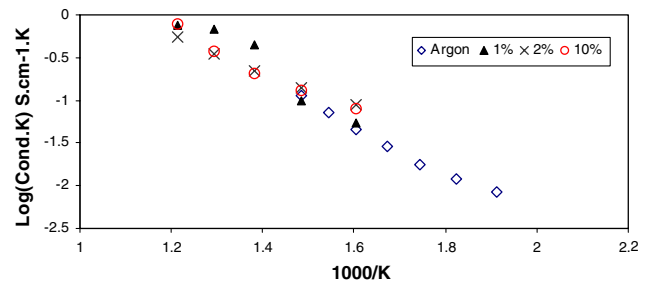


Fig. 6 H₂S concentration dependency of ionic conductivity versus temperature for 0.9CaS:Nd₂S₃. The legend gives the H₂S concentration in hydrogen in Vol.%

greater than 450 °C indicating ionic conductivity, Fig. 6. However at lower temperatures, conduction via positive holes occurs since an increased conductivity was observed as the hydrogen sulfide partial pressure was increased from 0 Vol.% (argon) to 1 Vol.% H₂S/Ar, Fig. 6. The filling of sulfur vacancies by sulfide ions from H₂S producing positive holes is described by Eq. 2. The conductivity of 0.8CaS:Nd₂S₃ decreases in the presence of a hydrogen sulfide partial pressures at all temperatures, indicating the presence of electronic conduction, Fig. 7. The formation of quasi-free electrons at low partial pressures may be expressed by Eq. 3.



where $V_{S^{2-}}$ —sulphide anion vacancy; S^{2-} —sulphur anion in unit cell.

The conductivity of 0.7CaS:Nd₂S₃ also decreases with increasing H₂S partial pressure, suggesting an electronic contribution to the conduction process, similar to 0.8CaS:Nd₂S₃.

Whilst performing impedance spectroscopy in various hydrogen sulfide concentrations differentiates ionic conduction from electronic, it does not explicitly confirm cationic conduction from anionic.

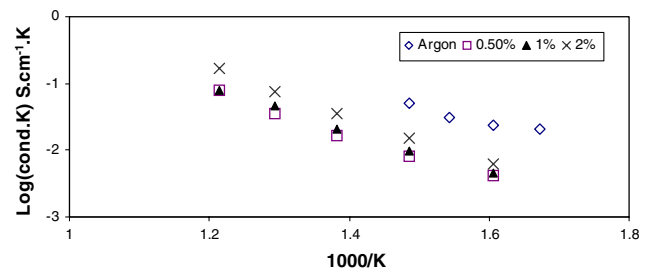


Fig. 7 H₂S concentration dependency of ionic conductivity versus temperature for 0.8CaS:Nd₂S₃. The legend gives the H₂S concentration in hydrogen in Vol.%

However, the Arrhenius plot of bulk conductivity gives the activation energy for the hopping process associated with ionic motion within a crystal lattice. Therefore low activation energy occurs for hopping with little resistance, such as small cations or for unit cells with short jump distances and hence small activation energies would favour the intuition of cation conduction. Since there are no published data for experimentally determined activation energies for sulfide ion conduction, except for CaS which only has thermally introduced vacancies, the activation energy (1.21–.96 eV) [22] for this process was reduced by the association energy of 0.5 eV [23–25] to develop a likely range of 0.61–1.66 eV to be used for comparison.

The larger sulfide ion is expected to move slower than the oxide ion at a given temperature and a similar lattice (fluorite) therefore the larger time constant (with respect to oxide ion conduction in YSZ) indicates anionic conduction in the doped CaNd_2S_4 series.

Conclusions

A series of solid solutions in the system $x\text{CaS}:\text{Nd}_2\text{S}_3$ were synthesised using solid state methods. Rietveld refinement of collected powder X-ray diffraction data show that the desired cubic Th_3P_4 type structure was formed.

The identifying feature of a pure ionic conductor is the presence of a low frequency ionic blocking arc in the Nyquist plot; this is only present for $0.9\text{CaS}:\text{Nd}_2\text{S}_3$. All other compounds in the series $x\text{CaS}:\text{Nd}_2\text{S}_3$ are at best mixed ionic–electronic conductors.

Varying the H_2S concentration from 0 Vol.% (pure Argon) to 10 Vol.% H_2S , confirmed $0.9\text{CaS}:\text{Nd}_2\text{S}_3$ to be an ionic conductor over this range of H_2S concentrations and at temperatures as low as 300 °C. Further doping to ($\geq 0.8\text{CaS}:\text{Nd}_2\text{S}_3$) resulted in electronic conduction, since a decrease in conduction occurred with the increase in H_2S concentration.

The activation energy for bulk conduction in the $x\text{CaS}:\text{Nd}_2\text{S}_3$ series lies within the probable range for sulfide ion conduction.

The bulk conductivity of $0.9\text{CaS}:\text{Nd}_2\text{S}_3$ using graphite electrodes and applying Jamnik's equivalent circuit model is $1.09 \times 10^{-6} \text{ Scm}^{-1}$ which agrees very well with data by Kalinina et al. derived from galvanic cell bulk conductivity measurements ($1.15 \times 10^{-6} \text{ Scm}^{-1}$).

The bulk conductivity depends on the model used, however, all models analysed identify $0.8\text{CaS}:\text{Nd}_2\text{S}_3$ as the compound with the maximum bulk conductivity. As $0.8\text{CaS}:\text{Nd}_2\text{S}_3$ bulk conductivity decreases with increasing H_2S partial pressure, the presence of electronic conduction is suggested.

The significant improvement in bulk conductivity though formation of solid solutions is confirmed since CaNd_2S_4 has a bulk conductivity significantly smaller than that of all the solid solutions analysed.

At high doping levels development of electronic conduction occurs.

References

1. Flahaut J, Guittard M, Patrie M, Pardo MP, Golabi SM, Domange L (1965) *Acta Cryst* 19:14
2. Andreev OV, Kislovskaia TM, Kertman AV (1990) *Zh Neorg Khim* 35:1280
3. Kalinina LA, Murin IV, Lyalina MY, Shirokova GI (1995) *Russ J Electrochem* 31:583
4. Kalinina LA, Fominykh EG, Tsirenova LS, Ushakova YN, Shirokova GI, Murin IV (2000) *Russ J Appl Chem* 73:1015
5. Worrell WL, Tare VB, Bruni FJ (1967) High temperature technology – proceedings of the third international symposium on high temperature technology, Stanford Research Institute, California
6. Carter FL (1972) *J Solid State Chem* 5(2):300
7. Eguchi K, Setoguchi T, Inoue T, Arai H (1992) *Solid State Ionics* 52:165
8. Inaba H, Tagawa H (1996) *Solid State Ionics* 83:1
9. Yahiro H, Eguchi K, Arai H (1989) *Solid State Ionics* 36:71
10. Yahiro H, Eguchi K, Arai H (1986) *Solid State Ionics* 21:37
11. Butler V, Catlow CRA, Fender BEF, Harding JH (1983) *Solid State Ionics* 8:109
12. Minervini L, Zacate MO, Grimes RW (1999) *Solid State Ionics* 116:339
13. Nagata K, Goto K (1974) *Metall Trans* 5:899
14. Vanderah TA, Lowe-Ma CK (1992) *J Am Ceram Soc* 75(7):1988
15. Ono K, Oishi T, Moriyama J (1981) *Solid State Ionics* 3/4:555
16. Bauerle JE (1969) *J Phys Chem* 30:2657
17. Jamnik J (2003) *Solid State Ionics* 157:19
18. Fleig J, Maier J (1996) *Solid State Ionics* 85:17
19. Fleig J (2000) *Solid State Ionics* 131:117
20. Jamnik J, Maier J, Pejovnik S (1999) *Electrochim Acta* 44:4139
21. Macdonald JR (1987) *Impedance spectroscopy*. Wiley, New York
22. Pandey R, Ghosh PK (1981) *Solid State Commun* 38:647
23. Nowick AS (2000) *Solid State Ionics* 136:1307
24. Nowick AS, Liang KC (2000) *Solid State Ionics* 129:209
25. Tschöpe A, Sommer E, Birringer R (2001) *Solid State Ionics* 139:295